

Hadronic bound-states in SU(2) from Dyson–Schwinger Equations

Milan Vujanovic^{1a} and Richard Williams^{2b}

¹ Institut für Physik, Karl-Franzens–Universität Graz, Universitätsplatz 5, 8010 Graz, Austria.

² Institut für Theoretische Physik, Justus-Liebig–Universität Giessen, 35392 Giessen, Germany.

Received: date / Revised version: date

Abstract. By using the Dyson-Schwinger/Bethe-Salpeter formalism in Euclidean spacetime, we calculate the ground state spectrum of $J \leq 1$ hadrons in an SU(2) gauge theory with 2 fundamental fermions. We show that the rainbow-ladder truncation, commonly employed in QCD studies, is unsuitable for a description of an SU(2) theory. This we remedy by truncating at the level of the quark-gluon vertex Dyson-Schwinger equation in a diagrammatic expansion. Results obtained within this novel approach show excellent agreement with lattice studies. These findings emphasize the need to use techniques more sophisticated than rainbow-ladder when investigating generic strongly interacting gauge theories.

PACS. 11.10.St - 12.38.Lg - 12.60.Rc

1 Introduction

Quantum Chromodynamics (QCD) is a strongly interacting gauge theory whose study has proven to be one of the most formidable challenges of modern theoretical physics. Whilst the high-energy regime of QCD is by now relatively well explored in terms of perturbation theory, the arguably more interesting (and intrinsically non-perturbative) phenomena such as dynamical chiral symmetry breaking and confinement are yet to be fully understood.

One of the strategies which might lead to our better understanding of QCD is to investigate theories which are QCD-like, but have certain properties that make them technically less challenging than QCD itself. A prime example is provided by studies of SU(2) gauge theories with an even number of fermion flavors. Lattice simulations of these theories at non-zero chemical potential do not suffer from the sign problem, and such models thus provide ideal conditions to study the phase diagram of strongly interacting matter [1–11].

Here we wish to concentrate on the situation with two fundamentally charged Dirac fermions [1, 8, 10, 11]. Such a theory may also be interesting in the context of a unified description of cold asymmetric Dark Matter (DM) and dynamical electroweak (EW) symmetry breaking [12–14], wherein the ground state hadronic spectrum at $T = 0$, $\mu = 0$ is of great importance. It is exactly this hadronic spectrum that will be the central focus of our study.

In this paper we use the non-perturbative, continuous and covariant formalism of Dyson-Schwinger (DSE)

and Bethe-Salpeter (BSE) equations in Euclidean spacetime [15–18]. When applied to QCD, the most common truncation one can make is that of rainbow-ladder (RL), wherein the quark-antiquark interaction kernel is replaced by a dressed one gluon exchange. It is the simplest approximation scheme that respects the axial-vector Ward-Takahashi identity (axWTI), thus preserving the chiral properties of the theory and the (pseudo)-Goldstone boson nature of light pseudoscalar mesons. With a judicious choice of model dressing functions, the RL truncation has been applied relatively successfully to QCD phenomenology for both mesons [19–31] and baryons [32–36].

However, as we will show in this paper, the RL truncation performs rather poorly when adapted to an SU(2) theory with 2 fundamental flavors, even though the theory is expected to have QCD-like dynamics. We discuss possible reasons for this in more detail in Section 2. Here we only comment that we strongly believe that (most) of the inadequacy of RL method comes from its weak connection to the underlying gauge sector. Remediating this requires the use of beyond rainbow ladder (BRL) techniques, with our preference towards those based on the diagrammatic expansion of quark-gluon vertex DSE [37–48]. Whilst there are other BRL methods available [49–55], we choose the diagrammatic approach as it makes it easier to study the influence of the gauge sector on hadronic observables. Our aim in this paper is thus not only to provide a continuum calculation complementary to the lattice investigations of [12, 13], but also to explicitly demonstrate the importance of using BRL methods when studying generic strongly interacting theories.

^a e-mail: milan.vujanovic@uni-graz.at

^b e-mail: richard.williams@theo.physik.uni-giessen.de

This manuscript is organised as follows. In Section 2 we discuss the DSEs relevant for our calculation, and also describe in some detail the approximations and model inputs we employ. In Section 3 we describe the extrapolation procedures used to obtain hadron masses, and provide estimates for errors coming from extrapolation. The results are discussed and compared to relevant lattice data in Section 4. We conclude in Section 5.

2 Framework

In a theory with 2 colors, both mesons and baryons (di-quarks) can be described in terms of a two-body Bethe–Salpeter equation. For the meson

$$[\Gamma_M(p, P)]_{ij} = \int_k [K(p, k, P)]_{ik;lj} [\chi_M(k, P)]_{kl}, \quad (1)$$

where \int_k stands for $\int d^4k/(2\pi)^4$ and $\Gamma_M(p, P)$ is the meson amplitude with appropriate J^{PC} quantum numbers, relative momentum p and total momentum P , and the meson wavefunction is $\chi_M(k, P) = S(k_+) \Gamma_M(k, P) S(k_-)$. The quark propagators are $S(k_\pm)$, at momenta $k_+ = k + \eta P$ and $k_- = k + (1 - \eta)P$, with k the loop momentum and $\eta \in [0, 1]$ the momentum partition factor. In a covariant study, the results are independent of η ; for concreteness, we work with $\eta = 1/2$. The final ingredient in Eq. (1) is the quark-antiquark 4-point interaction kernel $K(p, k, P)$. A diagrammatic representation of Eq. (1) for mesons is given in Fig. 1.

In order to solve the BSE, one clearly needs as input the quark propagator $S(p)$. This Green’s function is decomposed as

$$S^{-1}(p) = Z_f^{-1}(p^2) [i\not{p} + M(p^2)], \quad (2)$$

with $Z_f(p^2)$ the quark wavefunction and $M(p^2)$ the dynamical quark mass. The tree-level form is given by $S_0^{-1}(p) = i\not{p} + Z_m m$, where Z_m is the quark mass renormalisation constant. The quark propagator satisfies its own DSE, see Fig. 2, and is given by

$$S^{-1}(p) = Z_2 S_0^{-1}(p) + g^2 Z_{1f} C_F \int_k \gamma^\mu S(k+p) \Gamma^\nu(k+p, p) D_{\mu\nu}(k). \quad (3)$$

Here, $\Gamma^\nu(p, k)$ and $D_{\mu\nu}(k)$ are the full quark-gluon vertex and gluon propagator, respectively. Renormalisation constants of the quark field and quark-gluon vertex are Z_2 and

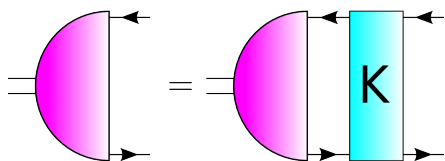


Fig. 1. The Bethe–Salepeter equation for the meson.

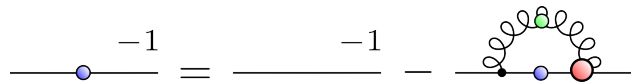


Fig. 2. The Dyson–Schwinger equation for the quark propagator.

Z_{1f} . They are related through a Slavnov–Taylor identity which takes a simple form when employing a miniMOM scheme [56] in Landau gauge, $Z_{1f} = Z_2/\tilde{Z}_3$ with \tilde{Z}_3 the renormalisation of the ghost propagator.

The 4-point interaction kernel $K(p, k, P)$ of Eq. (1) is connected to the self-energy part $\Sigma(p)$ of quark propagator DSE through the axial-vector Ward–Takahashi identity (axWTI)

$$[\Sigma(p_+) \gamma_5 + \gamma_5 \Sigma(p_-)]_{ij} = \int_k [K(p, k, P)]_{ik;lj} [\Sigma(k_+) \gamma_5 + \gamma_5 \Sigma(k_-)]_{kl}. \quad (4)$$

This identity encodes the chiral properties of the theory, and severely constrains the form of the BSE interaction kernel once an approximation for the quark DSE has been chosen. A direct connection is provided through the action of ‘cutting’ internal quark lines [37, 38].

2.1 Rainbow-ladder

The ‘rainbow’ part of RL truncation refers to the replacement of the full quark-gluon vertex in Eq. (3) by

$$\Gamma^\nu(k+p, p) \rightarrow \lambda(k^2) \gamma^\nu, \quad (5)$$

i.e. its tree-level form augmented by a model dressing function, $\lambda(k^2)$, that is a function of the gluon momentum alone. The corresponding axWTI-preserving approximation for BSE kernel is that of one gluon exchange (the ‘ladder’), which we show diagrammatically in Fig. 3.

In the RL approach, the model dressing function $\lambda(k^2)$ of Eq. (5) is often combined with the dressing of the gluon propagator $D_{\mu\nu}(k^2)$ into a single model function, constructed to reproduce correctly some hadronic observables, usually m_π and f_π . Whilst this method has shown considerable success in QCD phenomenology (see e.g. [57, 58] for some of the limitations of the model), in an SU(2) theory the approach fails badly even for light mesons with spin $J \leq 1$: see Table 2 for details.

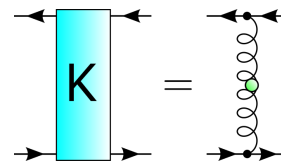


Fig. 3. The truncated two-body kernel in rainbow-ladder approximation.

There are two primary reasons why RL will not perform satisfactorily in a generic strongly-interacting theory. One reason is with regards to its very limited interaction structure ($\gamma^\nu \times \gamma^\mu$) which offers no variation in interaction strength across different meson channels. The second is that the connection to the underlying gauge dynamics is typically lost in the construction of an effective quark-gluon interaction; this prevents adequate rescaling of parameters such as $g^2 N_c$ that cannot be translated into a re-parameterization of an effective model.

2.2 Beyond rainbow-ladder

A BRL approach which is well suited for studying the influence of underlying Yang-Mills sector on the hadronic observables is based on the quark-gluon vertex [42, 44, 46, 48, 59–64]. Here, we focus on the truncated form of the DSE [48] shown in Fig. 4. Within this approximation, only the so-called non-Abelian (NA) diagram is kept in the quark-gluon vertex self-energy. The truncated kernel, consistent with constraints from chiral symmetry, is shown in Fig. 5.

So that the Bethe-Salpeter equation can be tackled, the evaluation of a fully self-consistent quark-gluon vertex is not performed. That is, the full calculated vertex (denoted by a red filled circle in Fig. 4) is not back-coupled into the non-Abelian diagram. Instead, the internal vertices (orange squares in Fig. 4) are modelled by the Eq. (5) with $\lambda(k^2)$ constructed such that it strongly resembles the tree-level projection of the full quark-gluon vertex at each iteration step; essentially, it depends upon a function $\Lambda(M_0)$ that encodes the interaction strength in terms of the dynamically generated quark mass. We used the parametrisation Eq. (21) of Ref. [48], with modifications that account for the change $N_c = 2$ and the rescaling of the gauge coupling g^2 ($g^2 N_c$ is left invariant). For $\Lambda(M_0)$ we use the functional form given in Eq. (22) of [48] with parameters $a \simeq 2.44$, $b \simeq 1.79$, $c \simeq -0.20$, $d \simeq 0.30$. The procedure described therein is used for solving the resultant coupled DSE system of a quark propagator and quark-gluon vertex.

We emphasize here that this model is, in a sense, highly constrained. Namely, once the input for the ghost and gluon propagators (which we will discuss shortly) and the truncation of the quark-gluon vertex DSE have been chosen, all other parts of the calculation are fixed. The BSE kernel follows from the axWTI, and the model dressing $\lambda(k^2)$ of Eq. (5) follows from the tree-level projection of the full quark-gluon vertex. We will re-iterate this point in

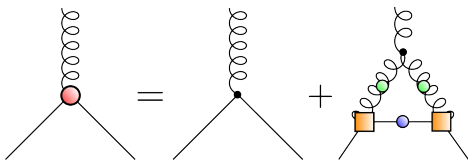


Fig. 4. The truncated DSE for the quark-gluon vertex.

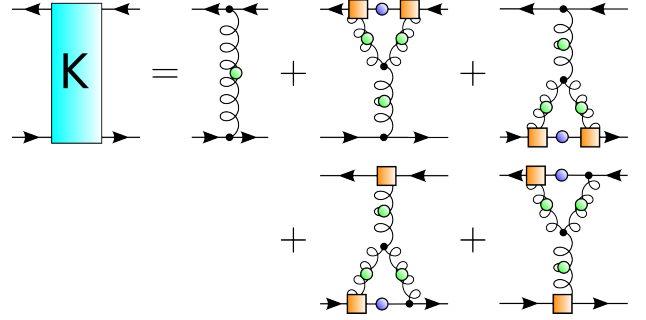


Fig. 5. The truncated two-body kernel beyond rainbow-ladder approximation.

Section 4.1, when we provide an estimation of the model dependence.

The final ingredient which we need to specify in our calculation is the gluon propagator $D_{\mu\nu}(k)$. We work in Landau gauge, where this Green’s function takes the form

$$D_{\mu\nu}(k) = T_{\mu\nu}(k) \frac{Z(k^2)}{k^2}, \quad (6)$$

with $T_{\mu\nu}(k) = \delta_{\mu\nu} - k_\mu k_\nu / k^2$ the transverse projector with respect to momentum k . The gluon dressing function which we use is plotted in Fig. 6. The details of this function and its parametrisation can be found in [65]. We point out that the gluon which we employ corresponds to a quenched DSE calculation. Ignoring the back-reaction of quarks onto the Yang-Mills sector is usually considered a good approximation for theories with QCD-like dynamics, as the corresponding effect on ‘observables’ like the chiral condensate, f_π and others is quite small [66]. However, the quenched approximation should be reconsidered in theories which have (nearly) conformal, or ‘walking’ dynamics. Walking dynamics arises naturally in models with a relatively large number of light fundamentally

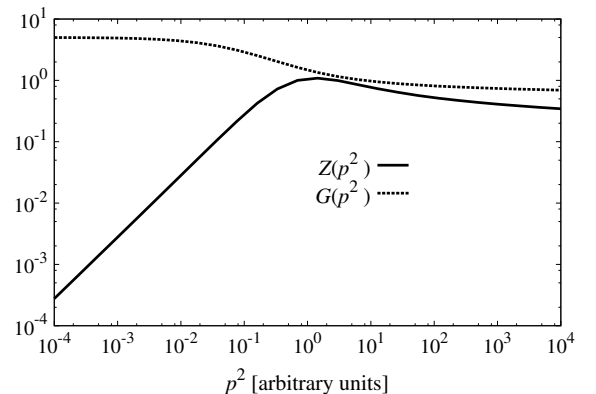


Fig. 6. Ghost (G) and gluon (Z) dressing functions employed in our calculations. The momentum p^2 is in arbitrary units: scale setting procedure is described in Section 4.2.

charged fermions [67–75], or fermions belonging to higher-dimensional representations of the gauge group [76–84].

3 Bound-states from space-like P^2

One of the consequences of working with Euclidean spacetime is that access to time-like quantities, such as masses of bound-states, requires an analytic continuation of the component Green’s functions to complex momenta. Whilst this is only a minor technicality thanks to many well-established techniques in the literature [23, 51, 85–87], there are situations in which existing methods do not apply, or which are simply too complicated to implement. In this case, indirect methods can be employed that enable access to a limited number of time-like quantities [88, 89].

In the next two sections we describe two techniques that have been widely used, and compare their performance in cases where direct analytic continuation is possible. This provides an estimate of the methods applicability to the study at hand.

3.1 Eigenvalue extrapolation

There are several means by which the mass spectrum of the BSE can be obtained. The most often used is through solution of Eq. (1), written as a matrix equation for simplicity

$$\Gamma_i = \lambda(P^2) K_{ij} \Gamma_j . \quad (7)$$

This has solutions at discrete values of the bound-state’s total momentum $P^2 = -M_i^2$. By introducing the function $\lambda(P^2)$ on the right, we obtain an eigenvalue equation whose bound-state solution correspond to $\lambda(P^2) = 1$.

Because Euclidean spacetime leads to the rest frame condition $P^\mu = (0, 0, 0, iM_i)$ we see that complex momenta will be probed whenever the mass is non-vanishing. However, since $\lambda(P^2)$ is a continuous function of P^2 , one can conceive that its continuation from spacelike $P^2 > 0$ to timelike $P^2 < 0$ may be obtained through appropriate function fitting and extrapolation.

It transpires, that performing a transformation of the eigenvalue [27]

$$g(\lambda) = 1 - \frac{1}{\lambda} , \quad (8)$$

removes a considerable degree of intrinsic curvature in the region close to the pole, rendering simple linear extrapolation viable, so long as we are ‘close’ by.

In the top panel of Fig. 7 we show the eigenvalue extrapolation of $\lambda(P^2)$ for various J^{PC} states. The data is first transformed via $g(\lambda)$, before a linear fit $f(P^2) = a + bx$ is performed. Finally, we plot the inverse function of g , $\lambda_{\text{fit}} = g^{-1}(f(P^2))$ as solid lines. Exact results, obtained via calculation in the complex plane, are included as labelled points.

3.2 Inverse vertex function extrapolation

The second means to obtain the mass spectrum employs instead the inhomogeneous BSE for the vertex function Γ_i

$$V_i = V_i^{(0)} + K_{ij} V_j . \quad (9)$$

The obvious difference between this and the homogeneous BSE is the inhomogeneous term $V_i^{(0)}$. Its introduction leads to several important changes to the solution. Setting the relative momentum p to zero, for convenience, we observe the appearance of poles

$$V_i(P^2) \sim \frac{1}{P^2 + M^2} , \quad (10)$$

as one approaches the bound-state $P^2 \sim -M^2$. Then, the determination of a bound-state mass is reduced to looking for zeros in $1/V_i$. Typically, the leading amplitude is used as point of reference, and one employs the method of bi-conjugate gradient (stabilised) for solution.

Restricting ourselves to spacelike momenta P^2 requires once more the use of fit functions and extrapolation. Here, the most useful are rational polynomials

$$R^{n,m}(x) = \frac{\sum_{i=0}^n a_i x^i}{1 + \sum_{i=1,m} b_i x^i} . \quad (11)$$

Note, that since the coefficients a_i, b_i are obtained through least-squares fitting, the resulting function is not a true Padé. Regardless, the procedure appears quite reliable as can be seen in the bottom panel of Fig. 7.

Table 1. Results for vertex pole extrapolation for QCD rainbow-ladder in the chiral limit, compared with the result computed through direct analytic continuation. All units are in MeV.

J^{PC}	calc	$R^{(2,2)}(L = 0.5)$	$R^{(2,2)}(L = 1.0)$
0^{-+}	0	1	1
0^{++}	658	657	656
1^{--}	738	731	728
1^{++}	900	899	899

We summarize our results for vertex pole approximation in Table. 1. In addition, we varied the fit range of P^2 to be $(0, L)$ (in GeV^2) with L given in the table. The results obtained with eigenvalue extrapolation are not quoted as the method performs rather poorly, especially in the 1^{++} channel, see top panel of Fig. 7.

4 Results

4.1 Estimation of model dependence

As already highlighted, the majority of model dependence stems from the truncation of the quark-gluon vertex DSE.

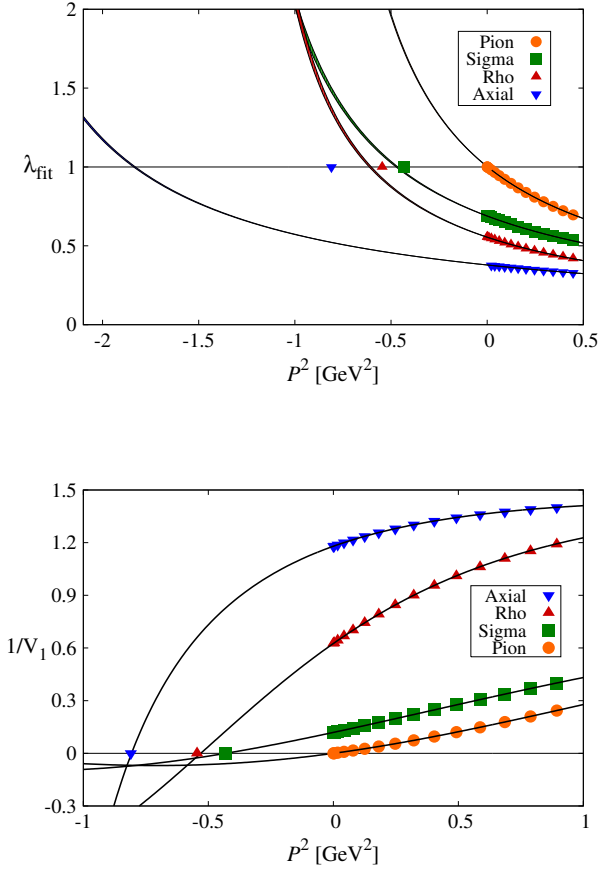


Fig. 7. Eigenvalue (*top*) and vertex pole (*bottom*) extrapolation from $P^2 > 0$ to the time-like region. The known result, obtained by direct analytic continuation, is given by labeled points for comparison.

Other parts of the calculation are constrained either by the underlying gauge dynamics (i.e. the ghost and gluon propagator which are taken from appropriate lattice or continuum calculations) or by chiral symmetry (in the process of truncating the BSE kernel). Thus, we can test the sensitivity of the truncation by varying the solution of the quark-gluon vertex within the constraints imposed by chiral symmetry breaking and the axWTI.

The natural step is to dress the three-gluon vertex. This is motivated by both the 3PI formalism [90] and through the effective resummation of neglected diagrams in the full DSE for the quark-gluon vertex. This in turn enables us to give a rough estimate as to the impact of including additional corrections on our results. It is sufficient to describe the full three-gluon vertex in Landau gauge by its tree-structure and one function of a symmetric variable $s_0 = (1/6) \cdot (p_1^2 + p_2^2 + p_3^2)$ [65]

$$\Gamma_{\mu\nu\rho}^{3g}(p_1, p_2, p_3) = \mathcal{A}(s_0) \cdot \Gamma_{\mu\nu\rho}^{(0)}(p_1, p_2, p_3). \quad (12)$$

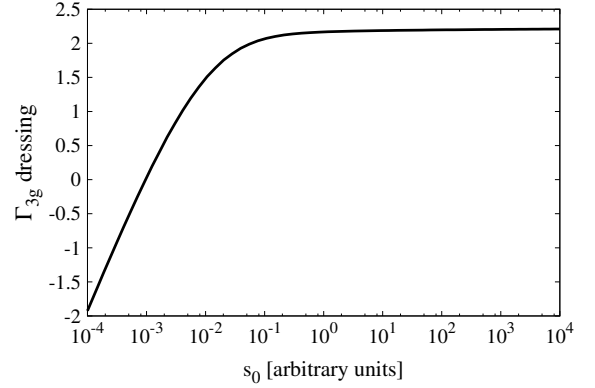


Fig. 8. Dressing for the three-gluon vertex, with $s_0 = (1/6) \cdot (p_1^2 + p_2^2 + p_3^2)$ and $a = s = 0$, see Eq. (50) of [65]. The momentum variable s_0 is in arbitrary units: scale setting procedure is described in Section 4.2.

The dressing function $\mathcal{A}(s_0)$ is obtained by solving the three-gluon vertex DSE in a ‘ghost triangle’ approximation, depicted in Fig. 9. The details of the calculation can be found in [65]. The resultant dressing function is shown in Fig. 8. Information available from continuum non-perturbative studies of the three-gluon vertex [65, 91–93] suggests that both the truncation of Fig. 9, and the restriction of possible tensor structures to the tree-level term, provide a reasonable phenomenological description of this Green’s function. The effect which the dressed three-gluon vertex has on the hadron masses can be seen in Table 2.

4.2 Discussion

Comparison of our results with the lattice [12, 13] requires the scale to be set by equating the electroweak (EW) scale with the pseudoscalar meson (‘pion’) decay constant, i.e. $v_{EW} = f_\pi = 246$ GeV. This puts the theory under investigation in the context of dynamical EW symmetry breaking, otherwise known as Technicolor (TC) [94, 95].

The drawbacks that the SU(2) model discussed here (and any other model with QCD-like dynamics) faces as a Technicolor template are by now well known. These include the problems with precision tests on flavor-changing

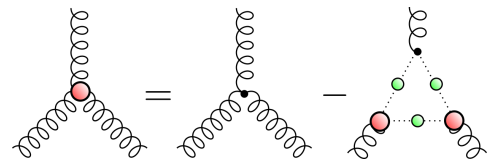


Fig. 9. The truncated DSE for the three-gluon vertex. To ensure that bose-symmetry is maintained the right-hand side is averaged over all cyclic permutations.

neutral currents [96], and the composite ‘Higgs boson’ which is expected to be very heavy. This latter problem is seen here, whereupon we do not find an isoscalar scalar (‘sigma’) meson (a TC version of the Higgs boson) below 1.43 TeV. This situation, however, might change drastically if one considers explicitly the couplings to Standard Model particles [97], or more general EW embeddings [98]. Another promising approach to Technicolor phenomenology is to use nearly conformal theories as Technicolor templates [99–102]. As we are presently concerned with the QCD-like aspects of the model under investigation, we will not comment on its possible Technicolor applications further.

Ground state masses for various J^{PC} mesons are shown for both the rainbow-ladder (RL) and beyond rainbow-ladder (BRL) truncations in Table 2, where they are additionally compared with the relevant lattice calculations. RL results were obtained by means of direct analytic continuation, whilst those of BRL were extrapolated from the region of spacelike P^2 via the inverse vertex function. Since in the BRL approach, complex plane calculations are not yet available [103], the pion decay constant is estimated from the dressing functions of the quark propagator [104]

$$f_\pi^2 = \frac{N_c}{4\pi^2} \int_0^\infty dy y \frac{M(y)Z_f(y)}{(y+M^2(y))^2} \left(M(y) - \frac{y}{2} \frac{dM(y)}{dy} \right), \quad (13)$$

with $y = p^2$ and $M(p^2)$, $Z_f(p^2)$ given in Eq. (2). The Pagels-Stokar formula of Eq. (13) is a chiral limit relation which is known to underestimate f_π by about ten percent [20, 105], since it ignores the sub-leading pion amplitudes. Because f_π is used to set the scale in our calculation, the meson masses obtained in the BRL approach are overestimated by about ten percent. This error due to scale setting is included in the results shown in Table 2, together with the uncertainty coming from the inverse vertex function method.

First, let us comment upon the RL vs BRL results in Table 2. In both cases the scale is set in the same way and color factors changed appropriately, yet the results differ by roughly a factor of two. This comes solely from there being no truly consistent means to rescale the product $g^2 N_c$ in a theory featuring a phenomenologically specified interaction constructed for QCD. Comparing the BRL result with lattice investigations, we see very good agreement, especially (perhaps accidentally) the central values for spin one mesons. However, since there are considerable error margins present in both cases, stronger statements about the agreement of our methods will have to wait for more refined calculations. For the spin zero mesons, lattice results will be made available in the near future. A calculation based on group theory scaling provides an estimate for the mass of the sigma meson in the model under consideration, with $m_\sigma \in [1, 1.5]$ TeV [97]. Our calculations of m_σ seem to favor the upper bound of this band, but it is encouraging to see that there are no large discrepancies present.

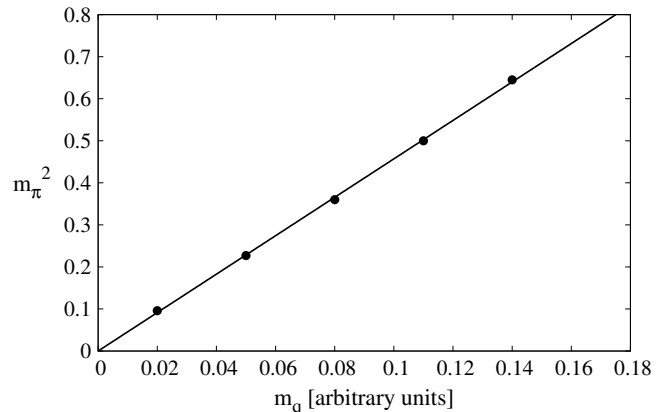


Fig. 10. Adherence of the calculated pion mass (squared) to the GMOR relation, as a function of the (corrected) quark mass m_q .

Regarding the continuum calculation, it seems that dressing of the three-gluon vertex does not change the meson masses significantly: the spin one mesons seem to be particularly robust in this respect. This leaves open the possibility that more elaborate modifications of our model (i.e. inclusion of additional diagrams and higher n -point Green’s functions in the quark-gluon vertex DSE) might not change the results appreciably. However, note that dynamical contributions that can collectively be termed ‘pion cloud’ effects are known to be important, and are the focus of present and future investigations.

Aside from the chiral limit study, we also performed calculations for non-vanishing current quark masses. In

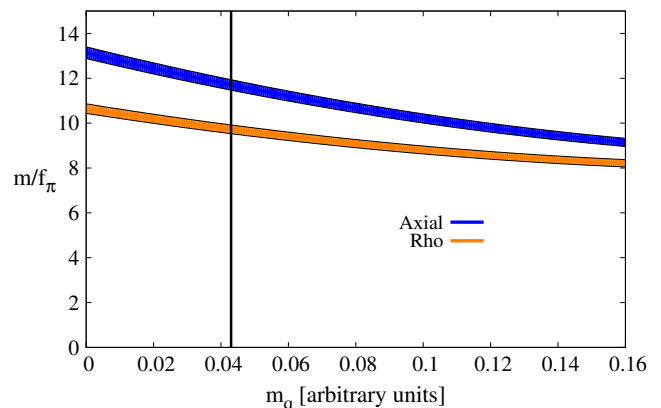


Fig. 11. $J = 1$ meson masses (in units of f_π) as a function of current quark mass. Bands correspond to uncertainties due to the extrapolation. The right-hand side of the vertical line corresponds to the region where $m_\rho \leq 2m_\pi$.

Table 2. Chiral limit results for meson masses in rainbow-ladder (RL) and beyond rainbow-ladder (BRL) truncations, compared with lattice data for an SU(2) theory. All units are in TeV. Errors of the BRL results are given in brackets, with the first number coming from uncertainties in the extrapolation procedure, and the second one due to an overestimation of the scale setting, see text for details. For the 0^{++} state, our continuum result is for an isoscalar; lattice results are forthcoming.

J^{PC}	RL	BRL, bare 3g vertex	BRL, dressed 3g vertex	Lattice, from [12, 13]
0^{-+}	0	0	0	–
0^{++}	0.88	1.63(8)(16)	1.42(6)(14)	–
1^{--}	1.38	2.66(12)(27)	2.53(8)(25)	2.5 ± 0.5
1^{++}	1.67	3.36(14)(34)	3.30(14)(33)	3.3 ± 0.7

Fig. 10 we demonstrate the validity of Gell-Mann-Oakes-Renner (GMOR) relation in the BRL approach, while in Fig. 11 we plot the masses of spin one mesons (in units of f_π) as a function of current quark mass. Both plots correspond to a calculation with a bare three-gluon vertex. The results shown in Fig. 11 seem to compare well with the ones shown in Fig. 6 of [13]; however, a direct comparison is not possible since we don’t have enough information to relate our m_q to the ones employed in [13]. One should also note that the relation of Eq. (13), which is used to evaluate f_π in all our calculations, becomes less reliable beyond the chiral limit.

As a final remark, we note that the calculation of the baryonic spectrum in this theory does not require any additional effort. An SU(2) gauge theory possesses an enlarged (Pauli-Gürsey) flavor symmetry, which implies that chiral multiplets will contain both mesons and baryons (diquarks). In other words, a meson with J^P quantum numbers will be degenerate with a J^{-P} diquark. This degeneracy (which breaks down if the chemical potential is raised above some critical value μ_c) has been confirmed in numerous lattice investigations [2, 4, 5, 12, 13].

5 Conclusions and outlook

We presented a Dyson-Schwinger/Bethe-Salpeter calculation of ground state hadron masses in a theory with two colors and two fundamentally charged Dirac fermions. We employed a novel beyond rainbow-ladder method and obtained good agreement with lattice results for spin one mesons: however, improved calculations will be needed to reduce uncertainties in both lattice and continuum approaches.

For $J = 0$ mesons, we demonstrated that chiral dynamics are satisfied (i.e. the GMOR relation holds) and obtained the mass of the sigma meson in good agreement with the analysis based on group theory scaling. Additionally, we showed a large discrepancy in results between rainbow-ladder and beyond rainbow-ladder methods, attributable to the fact that the factor $g^2 N_c$ cannot be rescaled consistently within the rainbow-ladder approach. This underlines the need to use more sophisticated techniques when studying generic non-Abelian gauge theories.

Besides masses, the beyond rainbow-ladder approach we outlined here can also be used to study hadronic de-

cays and form factors. A first step towards accessing these quantities is to extend the calculation to complex Euclidean momenta. However, the technical complications which arise are considerable and are subject to future investigation.

Acknowledgments

We would like to thank R. Alkofer, C. S. Fischer, A. Maas, H. Sanchis-Alepuz, and F. Sannino for useful discussions and a critical reading of this manuscript. This work was supported by the Helmholtz International Center for FAIR within the LOEWE program of the State of Hesse, a Lise-Meitner fellowship M1333–N16 from the Austrian Science Fund (FWF), and from the Doktoratskolleg “Hadrons in Vacuum, Nuclei and Stars” (FWF) DK W1203–N16. Further support by the European Union (Hadron Physics 3 project “Exciting Physics of Strong Interactions”) is acknowledged.

References

1. S. Hands, J. B. Kogut, M. P. Lombardo and S. E. Morrison, Nucl. Phys. B **558** (1999) 327 [hep-lat/9902034].
2. R. Aloisio, V. Azcoiti, G. Di Carlo, A. Galante and A. F. Grillo, Nucl. Phys. B **606** (2001) 322 [hep-lat/0011079].
3. R. Aloisio, V. Azcoiti, G. Di Carlo, A. Galante and A. F. Grillo, Phys. Lett. B **493** (2000) 189 [hep-lat/0009034].
4. S. Hands, I. Montvay, S. Morrison, M. Oevers, L. Scorzato and J. Skullerud, Eur. Phys. J. C **17** (2000) 285 [hep-lat/0006018].
5. J. B. Kogut, D. K. Sinclair, S. J. Hands and S. E. Morrison, Phys. Rev. D **64** (2001) 094505 [hep-lat/0105026].
6. S. Hands, I. Montvay, L. Scorzato and J. Skullerud, Eur. Phys. J. C **22** (2001) 451 [hep-lat/0109029].
7. J. B. Kogut, D. Toublan and D. K. Sinclair, Nucl. Phys. B **642** (2002) 181 [hep-lat/0205019].
8. S. Muroya, A. Nakamura and C. Nonaka, Phys. Lett. B **551** (2003) 305 [hep-lat/0211010].

9. B. Alles, M. D’Elia and M. P. Lombardo, Nucl. Phys. B **752** (2006) 124 [hep-lat/0602022].
10. S. Hands, S. Kim and J. I. Skullerud, Eur. Phys. J. C **48** (2006) 193 [hep-lat/0604004].
11. S. Cotter, P. Giudice, S. Hands and J. I. Skullerud, Phys. Rev. D **87** (2013) 3, 034507 [arXiv:1210.4496 [hep-lat]].
12. R. Lewis, C. Pica and F. Sannino, Phys. Rev. D **85** (2012) 014504 [arXiv:1109.3513 [hep-ph]].
13. A. Hietanen, R. Lewis, C. Pica and F. Sannino, JHEP **1407** (2014) 116 [arXiv:1404.2794 [hep-lat]].
14. A. Hietanen, R. Lewis, C. Pica and F. Sannino, arXiv:1308.4130 [hep-ph].
15. C. D. Roberts and A. G. Williams, Prog. Part. Nucl. Phys. **33** (1994) 477 [hep-ph/9403224].
16. R. Alkofer and L. von Smekal, Phys. Rept. **353** (2001) 281 [hep-ph/0007355].
17. C. S. Fischer, J. Phys. G **32** (2006) R253 [hep-ph/0605173].
18. I. C. Cloet and C. D. Roberts, Prog. Part. Nucl. Phys. **77** (2014) 1 [arXiv:1310.2651 [nucl-th]].
19. P. Maris, C. D. Roberts and P. C. Tandy, Phys. Lett. B **420** (1998) 267 [nucl-th/9707003].
20. P. Maris and C. D. Roberts, Phys. Rev. C **56** (1997) 3369 [nucl-th/9708029].
21. P. Maris and P. C. Tandy, Phys. Rev. C **60** (1999) 055214 [nucl-th/9905056].
22. P. Maris and C. D. Roberts, Int. J. Mod. Phys. E **12** (2003) 297 [nucl-th/0301049].
23. A. Krassnigg, PoS CONFINEMENT **8** (2008) 075 [arXiv:0812.3073 [nucl-th]].
24. A. Krassnigg, Phys. Rev. D **80** (2009) 114010 [arXiv:0909.4016 [hep-ph]].
25. M. Blank, A. Krassnigg and A. Maas, Phys. Rev. D **83** (2011) 034020 [arXiv:1007.3901 [hep-ph]].
26. A. Krassnigg and M. Blank, Phys. Rev. D **83** (2011) 096006 [arXiv:1011.6650 [hep-ph]].
27. M. Blank and A. Krassnigg, Phys. Rev. D **84** (2011) 096014 [arXiv:1109.6509 [hep-ph]].
28. H. L. L. Roberts, L. Chang, I. C. Cloet and C. D. Roberts, Few Body Syst. **51** (2011) 1 [arXiv:1101.4244 [nucl-th]].
29. C. S. Fischer, S. Kubrak and R. Williams, Eur. Phys. J. A **50** (2014) 126 [arXiv:1406.4370 [hep-ph]].
30. T. Hilger, C. Popovici, M. Gomez-Rocha and A. Krassnigg, arXiv:1409.3205 [hep-ph].
31. C. S. Fischer, S. Kubrak and R. Williams, arXiv:1409.5076 [hep-ph].
32. G. Eichmann, R. Alkofer, A. Krassnigg and D. Nicmorus, Phys. Rev. Lett. **104** (2010) 201601 [arXiv:0912.2246 [hep-ph]].
33. D. Nicmorus, G. Eichmann and R. Alkofer, Phys. Rev. D **82** (2010) 114017 [arXiv:1008.3184 [hep-ph]].
34. H. Sanchis-Alepuz, R. Alkofer, G. Eichmann and R. Williams, PoS QCD -TNT-II (2011) 041 [arXiv:1112.3214 [hep-ph]].
35. G. Eichmann, Phys. Rev. D **84** (2011) 014014 [arXiv:1104.4505 [hep-ph]].
36. H. Sanchis-Alepuz, R. Williams and R. Alkofer, Phys. Rev. D **87** (2013) 9, 096015 [arXiv:1302.6048 [hep-ph]].
37. H. J. Munczek, Phys. Rev. D **52** (1995) 4736 [hep-th/9411239].
38. A. Bender, C. D. Roberts and L. Von Smekal, Phys. Lett. B **380** (1996) 7 [nucl-th/9602012].
39. A. Bender, W. Detmold, C. D. Roberts and A. W. Thomas, Phys. Rev. C **65** (2002) 065203 [nucl-th/0202082].
40. P. Watson, W. Cassing and P. C. Tandy, Few Body Syst. **35** (2004) 129 [hep-ph/0406340].
41. P. Watson and W. Cassing, Few Body Syst. **35** (2004) 99 [hep-ph/0405287].
42. M. S. Bhagwat, A. Holl, A. Krassnigg, C. D. Roberts and P. C. Tandy, Phys. Rev. C **70** (2004) 035205 [nucl-th/0403012].
43. H. H. Matevosyan, A. W. Thomas and P. C. Tandy, Phys. Rev. C **75** (2007) 045201 [nucl-th/0605057].
44. R. Alkofer, C. S. Fischer, F. J. Llanes-Estrada and K. Schwenzer, Annals Phys. **324** (2009) 106 [arXiv:0804.3042 [hep-ph]].
45. C. S. Fischer and R. Williams, Phys. Rev. Lett. **103** (2009) 122001 [arXiv:0905.2291 [hep-ph]].
46. A. Windisch, M. Hopfer and R. Alkofer, Acta Phys. Polon. Supp. **6** (2013) 347 [arXiv:1210.8428 [hep-ph]].
47. M. Gomez-Rocha, T. Hilger and A. Krassnigg, arXiv:1408.1077 [hep-ph].
48. R. Williams, arXiv:1404.2545 [hep-ph].
49. C. S. Fischer, P. Watson and W. Cassing, Phys. Rev. D **72** (2005) 094025 [hep-ph/0509213].
50. C. S. Fischer, D. Nickel and J. Wambach, Phys. Rev. D **76** (2007) 094009 [arXiv:0705.4407 [hep-ph]].
51. C. S. Fischer, D. Nickel and R. Williams, Eur. Phys. J. C **60** (2009) 47 [arXiv:0807.3486 [hep-ph]].
52. C. S. Fischer and R. Williams, Phys. Rev. D **78** (2008) 074006 [arXiv:0808.3372 [hep-ph]].
53. L. Chang and C. D. Roberts, Phys. Rev. Lett. **103** (2009) 081601 [arXiv:0903.5461 [nucl-th]].
54. L. Chang and C. D. Roberts, Phys. Rev. C **85** (2012) 052201 [arXiv:1104.4821 [nucl-th]].
55. W. Heupel, T. Goecke and C. S. Fischer, Eur. Phys. J. A **50** (2014) 85 [arXiv:1402.5042 [hep-ph]].
56. L. von Smekal, K. Maltman and A. Sternbeck, Phys. Lett. B **681** (2009) 336 [arXiv:0903.1696 [hep-ph]].
57. G. Eichmann, R. Alkofer, I. C. Cloet, A. Krassnigg and C. D. Roberts, Phys. Rev. C **77** (2008) 042202 [arXiv:0802.1948 [nucl-th]].
58. S. x. Qin, L. Chang, Y. x. Liu, C. D. Roberts and D. J. Wilson, Phys. Rev. C **85** (2012) 035202 [arXiv:1109.3459 [nucl-th]].
59. J. Skullerud and A. Kizilersu, JHEP **0209** (2002) 013 [hep-ph/0205318].
60. J. I. Skullerud, P. O. Bowman, A. Kizilersu, D. B. Leinweber and A. G. Williams, JHEP **0304** (2003) 047 [hep-ph/0303176].
61. A. Kizilersu, D. B. Leinweber, J. I. Skullerud and A. G. Williams, Eur. Phys. J. C **50** (2007) 871 [hep-lat/0610078].

62. E. Rojas, J. P. B. C. de Melo, B. El-Bennich, O. Oliveira and T. Frederico, JHEP **1310** (2013) 193 [arXiv:1306.3022 [hep-ph]].
63. A. C. Aguilar, D. Binosi, D. Ibañez and J. Papavassiliou, Phys. Rev. D **90** (2014) 065027 [arXiv:1405.3506 [hep-ph]].
64. M. Mitter, J. M. Pawłowski and N. Strodthoff *in preparation*.
65. G. Eichmann, R. Williams, R. Alkofer and M. Vujanovic, Phys. Rev. D **89** (2014) 105014 [arXiv:1402.1365 [hep-ph]].
66. C. S. Fischer and R. Alkofer, Phys. Rev. D **67** (2003) 094020 [hep-ph/0301094].
67. W. E. Caswell, Phys. Rev. Lett. **33** (1974) 244.
68. T. W. Appelquist, D. Karabali and L. C. R. Wijewardhana, Phys. Rev. Lett. **57** (1986) 957.
69. T. Appelquist and L. C. R. Wijewardhana, Phys. Rev. D **36** (1987) 568.
70. T. Appelquist, G. T. Fleming and E. T. Neil, Phys. Rev. Lett. **100** (2008) 171607 [Erratum-ibid. **102** (2009) 149902] [arXiv:0712.0609 [hep-ph]].
71. F. Bursa, L. Del Debbio, L. Keegan, C. Pica and T. Pickup, Phys. Lett. B **696** (2011) 374 [arXiv:1007.3067 [hep-ph]].
72. A. Hasenfratz, Phys. Rev. Lett. **108** (2012) 061601 [arXiv:1106.5293 [hep-lat]].
73. A. Cheng, A. Hasenfratz and D. Schaich, Phys. Rev. D **85** (2012) 094509 [arXiv:1111.2317 [hep-lat]].
74. C.-J. D. Lin, K. Ogawa, H. Ohki and E. Shintani, JHEP **1208** (2012) 096 [arXiv:1205.6076 [hep-lat]].
75. M. Hopfer, C. S. Fischer and R. Alkofer, JHEP **1411** (2014) 035 [arXiv:1405.7031 [hep-ph]].
76. F. Sannino and K. Tuominen, Phys. Rev. D **71** (2005) 051901 [hep-ph/0405209].
77. D. D. Dietrich, F. Sannino and K. Tuominen, Phys. Rev. D **72** (2005) 055001 [hep-ph/0505059].
78. D. D. Dietrich and F. Sannino, Phys. Rev. D **75** (2007) 085018 [hep-ph/0611341].
79. S. Catterall and F. Sannino, Phys. Rev. D **76** (2007) 034504 [arXiv:0705.1664 [hep-lat]].
80. A. Maas, JHEP **1105** (2011) 077 [arXiv:1102.5023 [hep-lat]].
81. T. DeGrand, Y. Shamir and B. Svetitsky, Phys. Rev. D **83** (2011) 074507 [arXiv:1102.2843 [hep-lat]].
82. F. Bursa, L. Del Debbio, D. Henty, E. Kerrane, B. Lucini, A. Patella, C. Pica and T. Pickup *et al.*, Phys. Rev. D **84** (2011) 034506 [arXiv:1104.4301 [hep-lat]].
83. Z. Fodor, K. Holland, J. Kuti, D. Negradi, C. Schroeder and C. H. Wong, Phys. Lett. B **718** (2012) 657 [arXiv:1209.0391 [hep-lat]].
84. T. DeGrand, Y. Shamir and B. Svetitsky, Phys. Rev. D **88** (2013) 5, 054505 [arXiv:1307.2425].
85. M. Gimeno-Segovia and F. J. Llanes-Estrada, Eur. Phys. J. C **56** (2008) 557 [arXiv:0805.4145 [hep-th]].
86. S. Strauss, C. S. Fischer and C. Kellermann, Phys. Rev. Lett. **109** (2012) 252001 [arXiv:1208.6239 [hep-ph]].
87. A. Windisch, M. Q. Huber and R. Alkofer, Acta Phys. Polon. Supp. **6** (2013) 3, 887 [arXiv:1304.3642 [hep-ph]].
88. M. S. Bhagwat, A. Hoell, A. Krassnigg, C. D. Roberts and S. V. Wright, Few Body Syst. **40** (2007) 209 [nucl-th/0701009].
89. S. M. Dorkin, L. P. Kaptari, T. Hilger and B. Kampfer, Phys. Rev. C **89** (2014) 3, 034005 [arXiv:1312.2721 [hep-ph]].
90. J. Berges, Phys. Rev. D **70** (2004) 105010 [hep-ph/0401172].
91. D. Binosi, D. Ibañez and J. Papavassiliou, Phys. Rev. D **87** (2013) 12, 125026 [arXiv:1304.2594 [hep-ph]].
92. A. C. Aguilar, D. Binosi, D. Ibañez and J. Papavassiliou, Phys. Rev. D **89** (2014) 085008 [arXiv:1312.1212 [hep-ph]].
93. A. Blum, M. Q. Huber, M. Mitter and L. von Smekal, Phys. Rev. D **89** (2014) 061703 [arXiv:1401.0713 [hep-ph]].
94. S. Weinberg, Phys. Rev. D **19** (1979) 1277.
95. S. Dimopoulos and L. Susskind, Nucl. Phys. B **155** (1979) 237.
96. E. Eichten and K. D. Lane, Phys. Lett. B **90** (1980) 125.
97. R. Foadi, M. T. Frandsen and F. Sannino, Phys. Rev. D **87** (2013) 9, 095001 [arXiv:1211.1083 [hep-ph]].
98. G. Cacciapaglia and F. Sannino, JHEP **1404** (2014) 111 [arXiv:1402.0233 [hep-ph]].
99. B. Holdom, Phys. Rev. D **24** (1981) 1441.
100. B. Holdom, Phys. Lett. B **150** (1985) 301.
101. T. Akiba and T. Yanagida, Phys. Lett. B **169** (1986) 432.
102. K. Yamawaki, M. Bando and K. i. Matumoto, Phys. Rev. Lett. **56** (1986) 1335.
103. H. Sanchis-Alepuz and R. Williams *in preparation*.
104. H. Pagels and S. Stokar, Phys. Rev. D **20** (1979) 2947.
105. R. Alkofer, P. Watson and H. Weigel, Phys. Rev. D **65** (2002) 094026 [hep-ph/0202053].